Science AAAS

Covariant Glacial-Interglacial Dust Fluxes in the Equatorial Pacific and Antarctica

Gisela Winckler, *et al.*

Science **320**, 93 (2008);
DOI: 10.1126/science.1150595

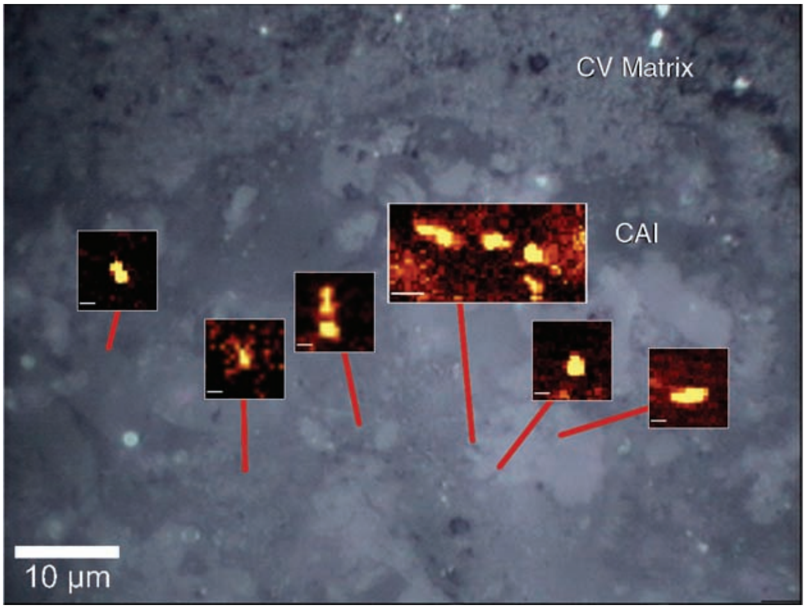

Fig. 3. Reflected light image of a polished Allende CAI surface with overlaid Raman images of the intensity of a Gaussian fit to the D* GW band. Scale bars for the inset images are 1 μm, except for the scale bar in the largest inset, which is 2 μm. Note the elongated nature of most of the whiskers. Whiskers that appear rounded may be truncated by polishing, may be oriented perpendicular to the sample surface, or may actually have a conical morphology.

the protoplanetary disk, very near the young Sun (*16*) and during a period when its polar and X-wind outflow may have been active (*17*, *18*). From here, these GWs could have been ejected from the young stellar system into interstellar space, producing an example of GW production and expulsion that may be extrapolated onto other young stellar systems. Furthermore, condensation of material ejected during supernovae may also produce GWs in a mechanism similar to that shown in meteorites.

In astronomy, whisker (or needle) morphologies of carbon, silicates, or iron have been invoked to explain several phenomena. They have been used to model the observed attenuation of IR light in the 3- to 9-μm range in observations of the galactic center and Cassiopeia A (*19–22*) that cannot be adequately explained by populations of polycyclic aromatic hydrocarbons and spherical silicates, iron, and graphite grains (*23*, *24*). Whiskers have been proposed to explain the apparent dimming of type Ia supernovae (SN Ia) and also for attenuating cosmic microwave background radiation (*21*, *22*, *25–27*), although the latter interpretation has been challenged (*28*). In the case of IR dimming of SN Ia, models invoking spherical (or "gray") dust show that the extinction of light in visible wavelengths would occur before dimming in the near IR (*29*, *30*). However, it has been calculated that inclusion of GWs at a concentration as low as 0.1% would produce the observed dimming without obstructing visible wavelengths (*31*, *32*). With the discovery of GWs in a meteoritic setting, their physical properties are now available for testing against these models and observations. Optical effects from these whiskers may have implications for interpreting data on supernova brightness that have been used to support the notion of dark energy (*33*, *34*).

References and Notes

1. T. Henning, F. Salama, *Science* **282**, 2204 (1998).
2. J. A. Jaszczak *et al.*, *Can. Mineral.* **45**, 379 (2007).
3. J. A. Jaszczak *et al.*, *Carbon* **41**, 2085 (2003).
4. S. Amelinckx *et al.*, *J. Cryst. Growth* **121**, 543 (1992).
5. R. Bacon, *J. Appl. Phys.* **31**, 283 (1960).
6. Y. Gogotsi *et al.*, *Science* **290**, 317 (2000).
7. G. Sears, *J. Chem. Phys.* **31**, 358 (1959).
8. P. H. Tan *et al.*, *Phys. Rev. B* **64**, 214301 (2001).
9. P. H. Tan *et al.*, *Philos. Trans. R. Soc. London Ser. A* **362**, 2289 (2004).
10. J. Dong *et al.*, *Appl. Phys. Lett.* **80**, 3733 (2002).
11. S. Dimovski, Y. Gogotsi, in *Nanotubes and Nanofibers*, Y. Gogotsi, Ed. (Taylor and Francis, New York, 2006), pp. 109–134.
12. Y. Saito, T. Arima, *Carbon* **45**, 248 (2007).
13. C. A. Johnson *et al.*, *Geochim. Cosmochim. Acta* **54**, 819 (1990).
14. A. N. Krot, E. R. D. Scott, M. E. Zolensky, *Meteoritics* **30**, 748 (1995).
15. F. E. Brenker, A. N. Krot, *Am. Mineral.* **89**, 1280 (2004).
16. L. Grossman, *Geochim. Cosmochim. Acta* **36**, 597 (1972).
17. F. Shu *et al.*, *Astrophys. J.* **429**, 781 (1994).
18. F. Shu *et al.*, *Science* **277**, 1475 (1997).
19. E. Dwek, *Astrophys. J.* **607**, 848 (2004).
20. E. Dwek, *Astrophys. J.* **611**, L109 (2004).
21. A. N. Aguirre, *Astrophys. J.* **512**, L19 (1999).
22. A. N. Aguirre, *Astrophys. J.* **525**, 583 (1999).
23. A. Li, B. T. Draine, *Astrophys. J.* **550**, L213 (2001).
24. V. Zubko *et al.*, *Astrophys. J. Suppl. Ser.* **152**, 211 (2004).
25. J. V. Narlikar *et al.*, *Publ. Astron. Soc. Pac.* **114**, 1092 (2002).
26. N. C. Wickramasinghe, F. Hoyle, *Astrophys. Space Sci.* **213**, 143 (1994).
27. A. N. Aguirre, *Astrophys. J.* **533**, 1 (2000).
28. C. Sivaram, G. A. Shah, *Astrophys. Space Sci.* **117**, 199 (1985).
29. A. Li, *Astrophys. J.* **584**, 593 (2003).
30. A. R. Robaina, J. Cepa, *Astron. Astrophys.* **464**, 465 (2007).
31. N. C. Wickramasinghe, D. H. Wallis, *Astrophys. Space Sci.* **240**, 157 (1996).
32. F. Hoyle *et al.*, *Astrophys. Space Sci.* **103**, 371 (1984).
33. S. Perlmutter *et al.*, *Astrophys. J.* **517**, 565 (1999).
34. A. G. Reiss *et al.*, *Astron. J.* **116**, 1009 (1998).
35. We thank A. Boss, G. Cody, T. Gooding, M. Hutson, A. Roberge, V. Rubin, A. Ruzicka, T. McCoy, E. Vicenzi, S. Rinehart, A. Weinberger, L. Welzenbach, and P. Tan for assistance; the NASA Sample Return Laboratory Instrument and Data Analysis Program, Astrobiology Science and Technology for Exploring Planets, and Astrobiology Institute programs for funding this work; the Antarctic Search for Meteorites expedition; and the RRUFF Raman database project.

29 November 2007; accepted 14 February 2008
Published online 28 February 2008;
10.1126/science.1153578
Include this information when citing this paper.

Covariant Glacial-Interglacial Dust Fluxes in the Equatorial Pacific and Antarctica

Gisela Winckler,[1]* Robert F. Anderson,[1,2] Martin Q. Fleisher,[1] David McGee,[1,2] Natalie Mahowald[3]

Dust plays a critical role in Earth's climate system and serves as a natural source of iron and other micronutrients to remote regions of the ocean. We have generated records of dust deposition over the past 500,000 years at three sites spanning the breadth of the equatorial Pacific Ocean. Equatorial Pacific dust fluxes are highly correlated with global ice volume and with dust fluxes to Antarctica, which suggests that dust generation in interhemispheric source regions exhibited a common response to climate change over late-Pleistocene glacial cycles. Our results provide quantitative constraints on the variability of aeolian iron supply to the equatorial Pacific Ocean and, more generally, on the potential contribution of dust to past climate change and to related changes in biogeochemical cycles.

Dust affects climate, both directly by altering the radiation budget of the atmosphere (*1*) and indirectly by influencing the biological uptake of CO_2 by the oceans (*2*) and the exchange of radiatively active gases with the atmosphere (*3*). Thus, dust may have been an important player in climate change in the past and is potentially one in the future. Polar ice core records [e.g., (*4*)] provide evidence that glacial dust deposition at high latitudes was as much as a factor of 25 higher than during interglacial periods. However, research on the role of dust in the past has been hampered by the scarcity of well-resolved internally consistent records of dust deposition at low latitudes (*5*), where changes may have important impacts on marine biogeochemistry (*6*), surface radiation (*7*), and the hydrological cycle (*8*).

Because of the potential importance of dust in forcing climate change, considerable effort is now devoted to including dust-generating processes in climate models (*9*–*11*). Complementary modeling endeavors to simulate the impact of dust deposition on marine biota, nutrient cycles, and atmospheric CO_2 (*6*, *12*). These impacts appear to be particularly important in high nutrient–low chlorophyll regions (HNLC) such as the equatorial Pacific Ocean, where concentrations of nutrients are high, yet chlorophyll, or primary production, is low. Phytoplankton growth in the equatorial Pacific has been shown to be limited by iron supply (*13*). Because aeolian dust is a substantial source of iron, changes in dust input have the potential to affect the ecosystem structure and carbon cycle in this iron-limited region.

Efforts to quantify dust-related impacts on climate and ocean biogeochemistry in the equatorial Pacific region have been limited by uncertainty as to the magnitude and even sign of glacial-interglacial dust flux changes. Several studies have reported increased dust fluxes during interglacial periods (*14*) or dust fluxes unrelated to glacial-interglacial cycles (*15*). Others have found dust accumulation maxima during glacial periods, as recently shown along short meridional transects in the eastern (*16*) and central (*17*) equatorial Pacific Ocean.

Here, we present a reproducible and self-consistent reconstruction of the aeolian dust flux across the equatorial Pacific from marine sediments deposited over the past 500,000 years. Our transect spans from the eastern equatorial Pacific [Ocean Drilling Program (ODP) site 849; 110.5°W, 0.2°N], across the central equatorial Pacific (TTN013-PC72; 0.1°N, 139.4°W), to the western equatorial Pacific (ODP site 806; 159.3°E, 0.3°N, RC17-177; 159.5°E, 1.75°N) (Fig. 1) (*18*). We use common thorium (^{232}Th), a trace element enriched in continental crust and low in basaltic volcanic material, as a tracer for lithogenic material, which, in remote regions in the Pacific Ocean, is predominantly derived from aeolian dust supply (*14*). A survey of circum-Pacific dust and loess data (*16*) shows that ^{232}Th concentrations in potential dust source areas fall within 1 part per million (ppm) of the average concentration of upper continental crust (10.7 ppm) (*19*). The validity of ^{232}Th as a dust proxy is supported by the linear relationships at three of our sites between ^{232}Th and terrigenous ^{4}He (fig. S1), an independent proxy for the lithogenic component that has been successfully used to reconstruct dust fluxes in marine sediments (*20*, *21*). Because ^{232}Th data are available at much higher resolution than ^{4}He in our cores, we focus here on ^{232}Th.

We evaluated dust fluxes by normalizing ^{232}Th concentrations to ^{230}Th. This approach relies on the observation that the flux of ^{230}Th to the sea floor approximately equals its known production rate from U decay in the overlying water column, thereby allowing the flux of any sedimentary constituent to be estimated from the ratio of the concentration of the constituent to that of ^{230}Th [corrected for decay and detrital ^{230}Th (*18*)]. There is currently an intense debate over the best approach to determine fluxes in marine sediments (*22*, *23*). Equatorial Pacific dust fluxes presented here exhibit excellent internal consistency across a wide geographical region and very different productivity regimes, as well as consistency with global ice volume and with dust fluxes from Antarctica. The lack of consistency among earlier records reflects, in part, the limited age resolution of many previous records. In addition, variable preservation of $CaCO_3$ in equatorial Pacific sediments may have introduced systematic errors in δ^{18}O-based age models. The use of ^{230}Th-normalization greatly reduces the sensitivity of derived fluxes to such errors and this contributes to the consistency among the dust flux records presented here.

After conversion to dust mass fluxes by dividing by the average ^{232}Th concentration of upper continental crust (10.7 ppm) (*19*), our ^{232}Th-based Holocene dust fluxes can be cross-calibrated with modern observations from sediment trap studies (Table 1). Agreement between our estimates of Holocene dust fluxes and the sediment trap fluxes, derived from independent proxies, is excellent, with respect to both absolute fluxes and the observed west-east gradient. The west-east gradient in dust fluxes is also consistent with in situ observations of dust fluxes by aerosol collection (*24*).

Dust fluxes in the central and eastern equatorial Pacific are comparable, with slightly higher fluxes at the central Pacific location (Table 1 and Fig. 1). Dust fluxes at two locations in the western Pacific, both on (ODP site 806) and off (RC17-177) the equator, are similar to one another and are consistently a factor of 3.5 higher than in the central and eastern regions.

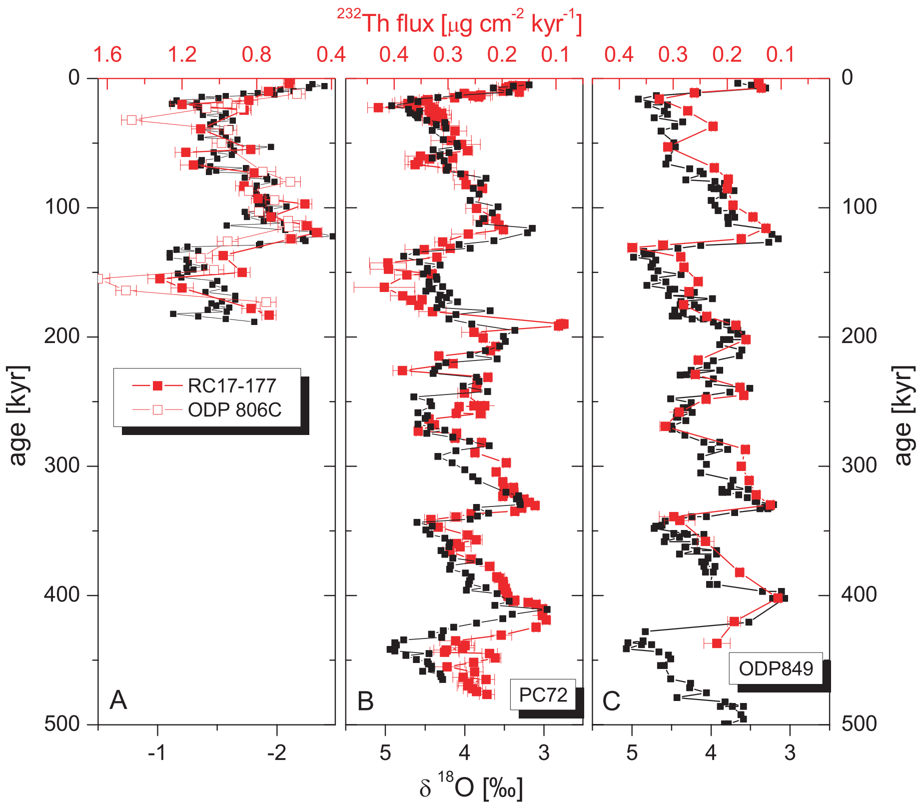

Fig. 1. Correlation of ^{232}Th fluxes (red, reverse scale) with global ice volume, as traced by the oxygen isotopic composition of foraminifera (black), for (**A**) ODP site 806C and RC17-177 in the western equatorial Pacific [Th isotope data from (*34*); planktonic δ^{18}O from (*35*)]; (**B**) TTN013-PC72 in the central equatorial Pacific [Th isotope data from (*17*) and from this study; benthic δ^{18}O from (*15*)], (**C**) ODP site 849 from the eastern equatorial Pacific [Th isotope data from this study; benthic δ^{18}O from (*33*)]. ^{232}Th fluxes are highest at maximum glacial conditions (as indicated by maximum δ^{18}O) and lowest at minimal ice coverage. The limited resolution of the records does not allow us to decipher a lead-lag relationship between dust flux and ice volume change at terminations.

[1]Lamont-Doherty Earth Observatory of Columbia University, Palisades, NY 10964, USA. [2]Department of Earth and Environmental Sciences, Columbia University, New York, NY 10027, USA. [3]Department of Earth and Atmospheric Sciences, Cornell University, Ithaca, NY 14853, USA.

*To whom correspondence should be addressed. E-mail: winckler@ldeo.columbia.edu

Table 1. Observation- and model-based estimates of dust fluxes to the Equatorial Pacific.

Source of dust flux estimate	Western Eq. Pac. (160°E) [g m^{-2} yr^{-1}]	Central Eq. Pac. (140°W) [g m^{-2} yr^{-1}]	Eastern Eq. Pac. (110°W) [g m^{-2} yr^{-1}]	Reference
		MODERN		
		Observations		
^{232}Th-derived dust flux (Holocene)	0.55	0.16	0.13	This study
Sediment trap*	0.84			(*37*)
Sediment trap†		0.15		(*38*)
		Model simulations		
ECHAM3	0.0098	0.0037	0.0089	(*9*)
ECHAM4	0.0325	0.0196	0.0211	(*10*)
MATCH	0.059	0.05	0.043	(*39*)
Composite‡	0.107	0.123	0.116	(*3*)
CCSM-SOMB	0.098	0.34	0.59	(*11*)
		LGM		
		Observations		
^{232}Th-derived dust flux (LGM)	1.37	0.40	0.30	This study
		Model simulations		
ECHAM3	0.119	0.39	0.71	(*9*)
ECHAM4	0.049	0.056	0.106	(*10*)
CCSM-SOMBLGMT§	0.060	0.336	0.411	(*11*)

*Calculated using terrigenous = total – carbonate – opal – 1.8*organic C (≈organic matter). †Calculated from Ti fluxes, assuming [Ti] = 0.3% in terrigenous fraction. ‡Composite model, based on several dust models. §LGMT, Last Glacial Maximum total source.

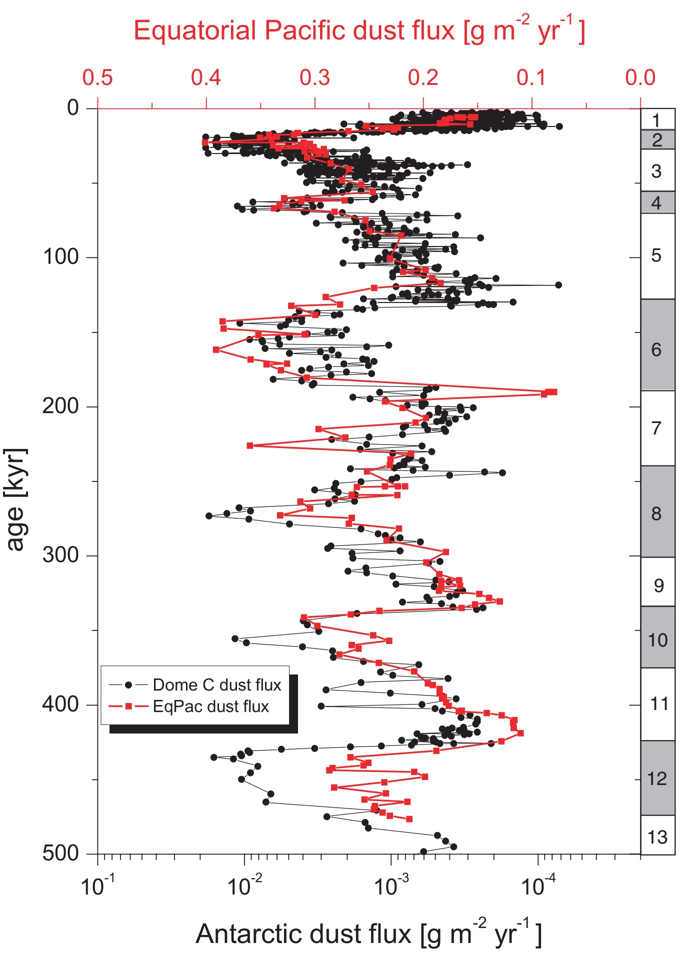

Fig. 2. Covariance of dust fluxes to the equatorial Pacific (TTN013-PC72, red) and Antarctica [European Project for Ice Coring in Antarctica (EPICA) site Dome C (EDC), black]. Dust fluxes at Dome C have been compiled from dust concentration data (*4*) and accumulation rates, derived from the new time scale EDC3 (*36*). Both records are plotted on their individual time scales [EDC3 (*36*) for the Dome C record; δ^{18}O-derived age model (*15*) for TTN013-PC72]. MIS indicated along the right age axis.

Throughout the past five glacial cycles, dust fluxes at all sites show striking correlation with δ^{18}O of foraminifera, which primarily tracks global ice volume (*25*). The amplitude of glacial-interglacial variations in dust fluxes, derived by comparing maximum (glacial) to minimum (interglacial) ^{232}Th fluxes (table S3), is consistent among all four locations, with glacial dust fluxes about a factor of 2.5 higher than interglacial fluxes. This indicates relatively uniform glacial/interglacial changes in dust regimes throughout the entire equatorial Pacific region, independent of the absolute dust flux levels.

The dust flux record from the equatorial Pacific is closely correlated to the dust flux reconstruction from Dome C in Antarctica (*4*) (Fig. 2). While the dust flux levels are much lower in Antarctica than in the tropics, and the relative glacial-interglacial variability of the tropical records is an order of magnitude smaller than for the polar record, the records show very similar behavior over five glacial cycles. Both records show the same rapid changes, such as the dust flux decrease over the last glacial termination. Even suborbital signals such as increased dust flux during marine isotope stage (MIS) 4 and the reversal in MIS 7 covary in the tropics and Antarctica.

The excellent correlation between dust fluxes recorded in the tropics and in Antarctica is particularly stunning given that the records from the two regions are based on different paleoarchives, and consequently independent age models, as well as different dust measures. Furthermore, the records represent at least three distinct source areas. Previous studies have found that most of the dust deposited in the western and central equatorial Pacific originates in Asia (*24*, *26*, *27*), whereas the dust deposited in the eastern equatorial Pacific is predominantly derived from sources in northern South America (*27*, *28*). Support for this source distribution comes from the regional patterns in the $^{4}He_{terr}$-^{232}Th characteristics (fig. S1), which point to similar dust sources for the west and central Pacific but suggest a distinct dust source for the eastern Pacific. The lower $^{4}He_{terr}/^{232}Th$ ratios at the eastern site are consistent with a dominant influence from a younger (^{4}He-poor) dust source of northern South America. The dominant source for dust reaching Antarctica is Patagonia (*29*).

The similar glacial-interglacial amplitude in deposition of dust from Asia (as seen in the western and central equatorial Pacific) and northern South America (as recorded in the eastern equatorial Pacific site) indicates quantitatively similar environmental responses to climate variability by dust mobilization processes in these low- and mid-latitude climate regions. Local processes affecting dust production appear to be subsidiary. In contrast, the much larger glacial dust flux increase in Antarctica (i.e., increase by a factor of 25 in Antarctica versus a factor of 2.5 in the tropical Pacific) suggests that local processes in Patagonia may have amplified dust generation in this source region. Specifically, the advance of

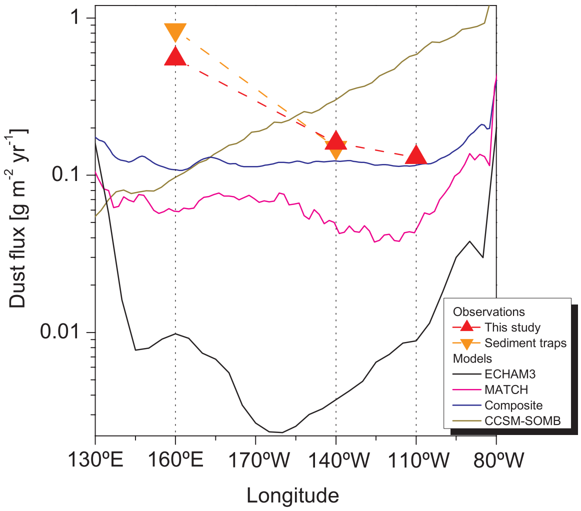

Fig. 3. Zonal gradients in dust fluxes across the equatorial Pacific from various recent model simulations (solid lines) and observations from sediment cores and traps (triangles). Model results are listed in chronological order of their publication: European Centre Hamburg Model 3 (ECHAM3) [black, (*9*)], Model of Atmospheric Transport and Chemistry (MATCH) [pink, (*39*)], Composite [blue, (*3*)], and Community Climate System Model–Slab Ocean Model with Biome3 sources (CCSM-SOMB) [olive, (*11*)]. The west-east decrease in the observations is not reflected by most dust models and is the reverse of the strong west-east increase in the most recent model simulation (*11*).

the Patagonian ice sheet during glacial periods, which increased glacial erosion and deposition of fine-grained glaciogenic sediments in extensive outwash plains, provided enhanced availability of dust to be exported to Antarctica (*30*). This ice sheet–driven amplifier of dust production is less relevant for tropical and mid-latitude dust sources because of the absence or limited size of ice sheets in these regions.

Three factors have been identified to explain higher dust fluxes in glacial periods compared with interglacials: a less vigorous hydrological cycle resulting in reduced washout, increased glacial wind intensities leading to increased dust entrainment, and expanded dust source areas [see (*31*) for a review]. Although there is uncertainty concerning the complex interplay of the factors influencing dust generation in any particular region, we infer from the synchronous changes in dust fluxes seen in our records that in each of the source areas, that is, Asia, northern South America, and Patagonia, the dominant processes regulating dust generation experienced a coherent response to global climate change. This response is consistent with other substantial glacial-interglacial environmental changes, such as the near-synchronous interhemispheric termination of the last glaciation inferred from temperate mountain glacial records (*32*). By this scenario, the consistent dust flux variations among different source regions suggests that the interhemispheric synchronicity is not limited to the last termination but extends back over at least the last five glacial cycles.

The need for deeper understanding of the processes that regulate dust generation and transport is demonstrated by the discrepancies between measured dust fluxes and several state-of-the-art model simulations (Table 1 and Fig. 3). Improvement to models over the past decade have brought modeled dust fluxes into the appropriate magnitude ranges for the equatorial Pacific. However, most models predict dust fluxes that are either relatively uniform zonally or, as for the most recent simulation (*11*), increase from west to east, in stark contrast to the strong west-to-east decrease by a factor of 3.5 in ^{232}Th-based dust fluxes.

Discrepancies are even more apparent for the models simulating climate conditions at the Last Glacial Maximum (LGM). Earlier models (*9*) inferred LGM/modern dust flux ratios ranging from 12 to 105, greatly exceeding our glacial/interglacial dust flux ratio of 2.5, while a more recent dust simulation (*11*) produced dust fluxes during the LGM that are lower than under modern conditions, at odds with greater glacial dust fluxes inferred from the sediment records. The newer model (*11*) also produces LGM dust fluxes that increase from west to east by about a factor of 6, in strong contrast to the observed decrease by a factor of 3.5 in our ^{232}Th-based reconstruction.

Research on the role of tropical dust in climate variability, as well as in climate-related changes in marine ecosystems and biogeochemical cycles, has been limited until now by the lack of internally consistent well-resolved records of dust flux. Results presented here should help to better constrain models of dust generation and transport. In addition, the coherent responses of dust fluxes from widespread source regions will serve as a basis for new hypotheses linking dust fluxes to climate change.

References and Notes

1. I. Tegen, A. A. Lacis, I. Fung, *Nature* **380**, 419 (1996).
2. J. Martin, *Paleoceanography* **5**, 1 (1990).
3. T. D. Jickells *et al.*, *Science* **308**, 67 (2005).
4. EPICA Community Members, *Nature* **429**, 623 (2004).
5. K. E. Kohfeld, S. P. Harrison, *Earth Sci. Rev.* **54**, 81 (2001).
6. J. K. Moore, S. C. Doney, K. Lindsay, *Global Biogeochem. Cycles* **18**, 10.1029/2004GB002220 (2004).
7. N. M. Mahowald *et al.*, *Geophys. Res. Lett.* **33**, 10.1029/2006GL026126 (2006).
8. R. L. Miller, I. Tegen, J. Perlwitz, *J. Geophys. Res.* **109**, 10.1029/2003JD004085 (2004).
9. N. Mahowald *et al.*, *J. Geophys. Res.* **104**, 15895 (1999).
10. M. Werner *et al.*, *J. Geophys. Res.* **107**, 10.1029/2002JD002365 (2002).
11. N. M. Mahowald *et al.*, *J. Geophys. Res.* **111**, 10.1029/2005JD006653 (2006).
12. A. J. Watson, D. C. E. Bakker, A. J. Ridgwell, P. W. Boyd, C. S. Law, *Nature* **407**, 730 (2000).
13. K. H. Coale *et al.*, *Nature* **383**, 495 (1996).
14. D. K. Rea, *Rev. Geophys.* **32**, 159 (1994).
15. R. W. Murray, M. Leinen, D. W. Murray, A. C. Mix, C. W. Knowlton, *Global Biogeochem. Cycles* **9**, 667 (1995).
16. D. McGee, F. Marcantonio, J. Lynch-Stieglitz, *Earth Planet. Sci. Lett.* **257**, 215 (2007).
17. R. F. Anderson, M. Q. Fleisher, Y. Lao, *Earth Planet. Sci. Lett.* **242**, 406 (2006).
18. Materials and methods are available as supporting material on *Science* Online.
19. S. R. Taylor, S. M. McLennan, *The Continental Crust: Its Composition and Evolution* (Blackwell, Oxford, 1985).
20. D. B. Patterson, K. A. Farley, D. K. Norman, *Geochim. Cosmochim. Acta* **63**, 615 (1999).
21. G. Winckler, R. F. Anderson, P. Schlosser, *Paleoceanography* **20**, 10.1029/2005PA001177 (2005).
22. M. Lyle *et al.*, *Paleoceanography* **20**, 10.1029/2004PA001019 (2005).
23. R. Francois *et al.*, *Paleoceanography* **22**, 10.1029/2005PA001235 (2007).
24. J. M. Prospero, M. Uematsu, D. L. Savoie, in *Chemical Oceanography*, J. P. Riley, Ed. (Academic Press, New York, 1989), pp. 187–218.
25. W. F. Ruddiman, *Earth's Climate: Past and Present* (W. H. Freeman, New York, 2001).
26. L. A. Krissek, T. R. Janecek, *Proc. ODP Sci. Res.* **130**, 471 (1993).
27. S. Nakai, A. N. Halliday, D. K. Rea, *Earth Planet. Sci. Lett.* **119**, 143 (1993).
28. A. M. Stancin *et al.*, *Earth Planet. Sci. Lett.* **248**, 840 (2006).
29. I. Basile *et al.*, *Earth Planet. Sci. Lett.* **146**, 573 (1997).
30. A. J. Ridgwell, A. J. Watson, *Paleoceanography* **17**, 10.1029/2001PA000729 (2002).
31. S. P. Harrison, K. E. Kohfeld, C. Roelandt, T. Claquin, *Earth Sci. Rev.* **54**, 43 (2001).
32. J. M. Schaefer *et al.*, *Science* **312**, 1510 (2006).
33. A. C. Mix *et al.*, *Proc. ODP Sci. Res.* **138**, 371 (1995).
34. S. M. Higgins, R. F. Anderson, F. Marcantonio, M. Schlosser, M. Stute, *Earth Planet. Sci. Lett.* **203**, 383 (2002).
35. D. W. Lea, D. K. Pak, H. J. Spero, *Science* **289**, 1719 (2000).
36. F. Parrenin *et al.*, *Clim. Past* **3**, 19 (2007).
37. H. Kawahata, A. Suzuki, H. Ohta, *Deep Sea Res.* **47**, 2061 (2000).
38. J. Dymond, R. Collier, J. McManus, S. Honjo, S. Manganini, *Paleoceanography* **12**, 586 (1997).
39. C. Luo, N. M. Mahowald, J. del Corral, *J. Geophys. Res.* **108**, 10.1029/2003JD003483 (2003).
40. We thank U. Ruth for compiling the dust flux data from Dome C on the new EDC3 time scale, M. Werner for making the data for the ECHAM4 run available, and J. Schaefer and W. Broecker for constructive comments. This research used samples provided by the Ocean Drilling Program (ODP site 849) and the University of Rhode Island core repository (TTN013-PC72). Funding for this study was provided by the National Science Foundation (grant OCE 02-21333 to R.F.A. and G.W.). We thank the Earth Institute Advance Program for supporting N.M.'s visit to Columbia University through a Marie Tharp Fellowship. This is L-DEO contribution 7143.

Supporting Online Material
www.sciencemag.org/cgi/content/full/1150595
Materials and Methods
Fig. S1
Tables S1 to S3
References

17 September 2007; accepted 19 February 2008
Published online 28 February 2008;
10.1126/science.1150595
Include this information when citing this paper.